Densification and nanocrystallisation of sol-gel ZrO$_2$ thin films studied by surface plasmon polariton-assisted Raman spectroscopy

A. Brioude[1], F. Lequevre[2], J. Mugnier[2], C. Bovier[1], J. Dumas[1], and J. C. Plenet[1,a]

[1] Département de Physique des Matériaux, Université Claude Bernard Lyon1 CNRS UMR 5586, 43 boulevard du 11 Novembre, 69622 Villeurbanne Cedex, France
[2] Laboratoire de Physico-Chimie des Matériaux Luminescents, Université Claude Bernard Lyon1[b], 43 boulevard du 11 Novembre, 69622 Villeurbanne Cedex, France

Abstract. Very thin ZrO$_2$ films (few nanometers) have been prepared by sol-gel process. These films were deposited onto a stack of a thin silver layer evaporated on a glass substrate for Surface Plasmons Resonance (SPR) experiments. The first aim of this work is to study the high densification of the sol-gel films followed by the refractive index and thickness accurate measurements at each step of the annealing procedure, using an optical set-up based on SPR. Secondly, SPR excitation coupled with micro-Raman experiment has also been performed to determine the thin films structure depending on layer thickness. Finally, Conventional Transmission Electron Microscopy (CTEM) and High Resolution (HRTEM) studies have been conducted to check and complete Raman spectroscopy results. A discussion compares the optical results and the Transmission Electron Microscopy observations and shows that ultra thin layers structure is strongly depends on films thickness.

PACS. 42.79.-e Optical elements, devices, and systems – 78.30.-j Infrared and Raman spectra – 78.66.-w Optical properties of specific thin films – 81.20.Fw Sol-gel processing, precipitation

Introduction

The Surface Plasmon Polariton (SP_p) excited by evanescent waves on smooth metal surfaces and out-coupled in attenuated total reflection (ATR) configuration improves the limited sensitivity of backscattering Raman investigations when studying ultra thin films. Thus, SP_p-assisted Raman spectroscopy has been used to study many systems as molecular overlayers adsorbed on well defined metal surfaces [1–4]. The enhancement of the Raman intensity [5–7] is due to the amplification of the electromagnetic field at the metal-dielectric interface due to the SP_p electromagnetic resonance.

This enhancement can be obtained in the so-called Kretschmann geometry [8] which consists of a prism and a thin metal film covered by the dielectric which is to be studied. This set-up allows excitation of the metal-thin film interface SP_p using laser incident light coming through the prism. This resonant coupling occurs at a specific incident angle (θ_{ATR}). The exact value of θ_{ATR} depends on a relation between the wavelength of the incident light, the dielectric constants and thicknesses of each layers making up the samples [9].

In the first part, we describe sample preparation constituted by silver layer deposition and ZrO$_2$ very thin film preparation by the Sol-Gel (SG) process. Densification of ZrO$_2$ ultra-thin sol-gel films is studied, measuring the evolution of refractive index and thickness of the dielectric film after each annealing step. In the last part, we present Raman scattering spectroscopy results when studying two samples of different thicknesses. The estimated enhancement factor of the Raman scattering intensity (around 85) is due to the SP_p excitation and is sufficient to determine the ZrO$_2$ films phases. Transmission Electron Microscopy (TEM) observations are conducted on the same Zirconia layers in order to check and complete the optical and spectroscopic results respectively.

Samples preparation and heat treatment procedure

Thin silver films were electron-gun deposited onto a pre-cleaned glass (®Pyrex, optical index 1.472 at 514.5 nm) under vacuum of 10^{-6} torr. The deposited layer thickness (50 ± 0.5 nm) and the evaporation rate (0.5 nm/s) were measured by a quartz balance. This thickness was

^{a} e-mail: `plenet@dpm.univ-lyon1.fr`
^{b} CNRS UMR 5620

determined in order to improve the light coupling efficiency. The silver growth rate was determine to procedure a smooth metal surface [10,11]. Very thin ZrO_2 films have been prepared by SG route and deposited by a dip-coating method [12,13] onto the silver layer. The sol was obtained by mixing zirconium n-propoxide $[Zr(OC_3H_7)_4, 70\%$ solution in propanol (Fluka)] [14] with a stabilizer to prevent ZrO_2 precipitation. In this study, zirconium alkoxide was modified with acetylacetone (acacH) according to the exothermic reaction [15]:

$$Zr(n - OC_3H_7)_4 + acacH \rightarrow Zr(n - OC_3H_7)_3$$
$$+(acacH) + C_3H_7OH.$$
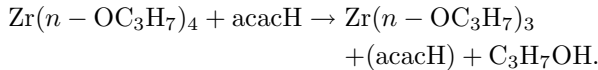
When the hydrolysis and condensation reactions have been performed, 2-propanol (Prolabo) was added to adjust the sol viscosity at the wanted value. This last step during the process was necessary to adjust the ultra thin films thickness in the range around few nanometers [16]. After the dip coating deposition, the films were dried at a temperature of 100 °C. Such films are continuous and crack free as proved by micro-optical observations. In this paper, we present results on three samples labelled A, B and C. As it has been presented above, film thicknesses are adjusted by addition of 2-propanol to the starting SG solution. The sample A and B has been obtained by diluting the sol with a volume ratio 6/1 for 2-propanol and sol respectively. In order to elaborate the thicker sample C, a 4/1 ratio has been selected. The sample A was annealed under Infra-Red (IR) lamp at a temperature around 750 °C under a pur O_2 flow. The total heat treatment duration was 28 minutes by step of 4 min mainly. This annealing time does not take into account the temperature rise time of about 10 seconds and the room temperature decrease of 1 minute. On the one hand, the aim of this annealing process by IR irradiation is to induce the nanocrystal growth into the film without destroying the silver layer and on the other hand to eliminate carbon residues due to SG method. The samples B and C were annealed for 15 minutes under IR lamp at a temperature around 500 °C under continuous pure O_2 flow and then were heat-treated in a tubular furnace under oxygen flow at 700 °C for 5 minutes. The aim of this last annealing treatment is to achieve crystallisation as it has been already shown elsewhere [17].

Thickness and refractive index measurement

A just dried SG film exhibits an amorphous structure [12,13]. Therefore, the aim of this study is to determine the crystallisation temperature for a well defined annealing procedure. Thicknesses and refractive index evolution of the sample A were measured using an SPR optical set-up already described in a previous paper [16]. These measurements presented in Figure 1 have been performed at a wavelength of 594.5 nm (He-Ne laser). Figure 1 shows that the ZrO_2 film refractive index strongly increases after a cumulative heat treatment of 8 min. During
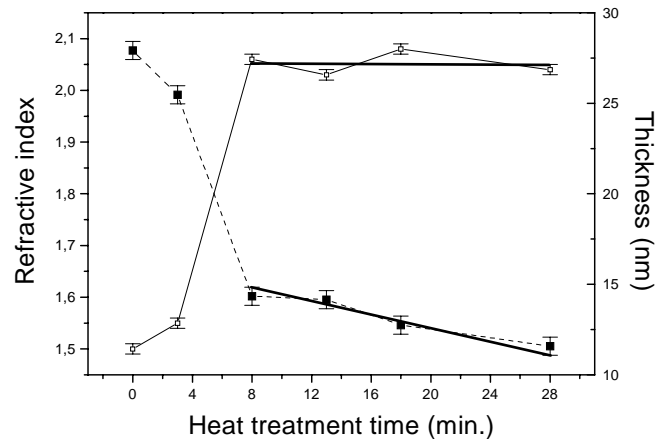

Fig. 1. Measured refractive index of sample A and corresponding thickness *versus* treatment annealing time.

the same time sample A thickness continuously decreases. A break in the slope of the two curves is observed, suggesting the onset of a phase transformation (see Fig. 1). After 8 min, the optical index of the sample A roughly remains constant, and its thickness just weakly decreases.

After a complete annealing treatment as described above the films thicknesses were 12 ± 0.5 nm and 26.6 ± 0.5 nm for the samples B and C respectively. Their refractive indices were 2.06 ± 0.01 and 1.92 ± 0.01 respectively confirming that the ultra-thin film refractive index is strongly dependant on the films thickness. Differences in their measured refractive indices have already been explained [18] and confirmed that the thinner the SG film is, the denser it is.

Transmission Electron Microscopy studies

In order to compare ZrO_2 ultra-thin films behaviour, and effects of annealing procedure, and thickness samples A, B, C have been analysed by electron microscopy. Conventional Transmission Electron Microscopy (CTEM) studies have been performed using a TOPCON EM-002B working at 200 kV to obtain the general picture on the changes in crystalline-phases. In this case ZrO_2 very thin films have been peeled off from their substrates and deposited onto a 3 mm copper grid for direct observation. Sample A CTEM analysis result is presented in Figure 2a. The associated diffraction pattern (Fig. 2b) shows that sample A exhibits a tetragonal phase (space groupe $P4_2/nmc$, [19]). It can be observed that the rings are not well-defined and not continuous. This means that the sample contains isolated nanocrystals so that only few crystalline orientations are detected in the diffraction pattern. The large diffuse and intense rings are the signature of the predominant amorphous phase. Due to the not well-resolved nanocrystals shape in the CTEM micrography, it is no possible to determine the mean diameter of each nanocrystal. Each dark zone contains several particles (see Fig. 2a). So an
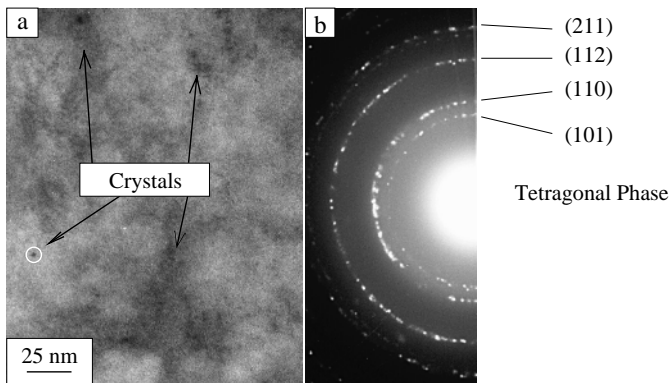
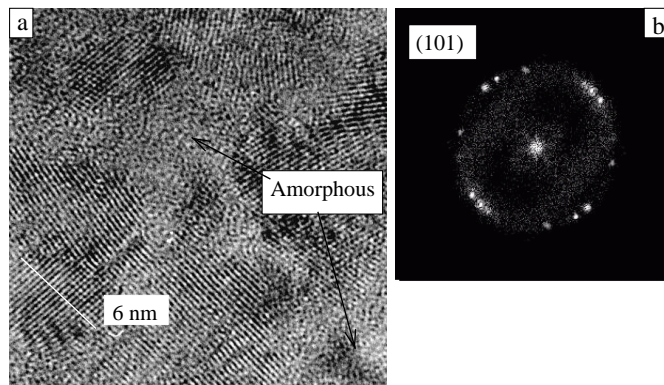**Fig. 2.** (a) Conventional Transmission Electron Microscopy image of sample A. (b) Associated diffraction pattern.

Fig. 4. (a) Conventional Transmission Electron Microscopy image of sample B. (b) Associated diffraction pattern.

Fig. 3. (a) High Resolution Transmission Electron Microscopy image of sample A. (b) Associated diffraction pattern.

Fig. 5. (a) Conventional Transmission Electron Microscopy image of sample C. (b) Associated diffraction pattern.

HRTEM study of the same area must be conducted and is presented in Figure 3a. This picture shows several crystals randomly oriented with sizes in the range between 5 to 10 nm. The corresponding Fourier transformation of this image is shown in Figure 3b with indexed points corresponding to (101) atomic planes. Taking into account that the film A is a mixture of an amorphous phase and of nanocristals, the difference between the measured refractive index and bulk one (2.05 and 2.20) [20, 21] respectively can be explained.

As films exhibit different refractive indices for the same heat treatment, their structures have been investigated by CTEM. CTEM analysis results are presented in Figures 4a and 5a respectively. The diffraction pattern associated with Figure 4a (sample (B)) shows clearly a mixture of characteristic rings for the tetragonal phase and the monoclinic one (space groupe $P2_1/c$). For sample (C) (Fig. 5b) the tetragonal phase is only observed. It is to notice that for thicker films used as planar optical waveguide and exhibiting a thickness in the range around 150 nm, monoclinic phase only appears at temperature annealing greater than 600 °C and for an annealing time of 1 hour [22, 23].
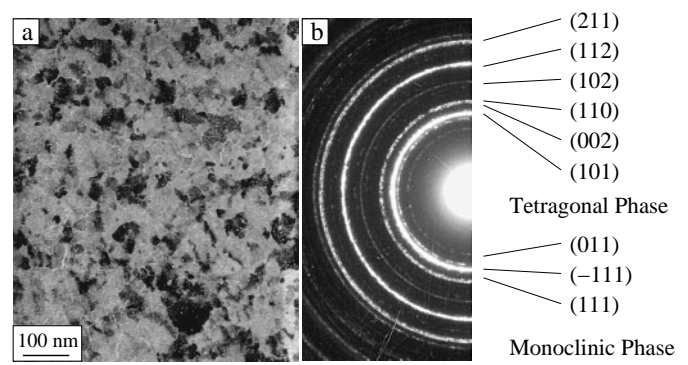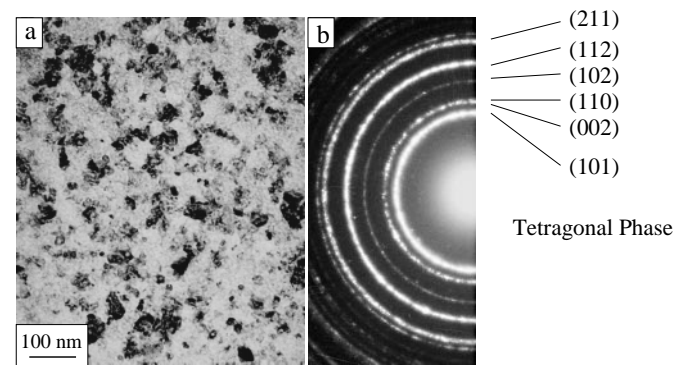
For sample B, annealing, temperature and duration required for the crystallisation are lower than for thicker films, thus the thermal behaviour of the SG films depends on their thicknesses. We have already observed this phenomenon for TiO₂ SG films [17].

Micro-Raman spectroscopy experiment

The device used to perform the Raman experiment is presented in Figure 6. The Raman scattering measurements were obtained with an XY Dilor triple spectrometer followed by a Nitrogen cooled CCD (Charge Coupled Device) multichannel detector. The 2016 type Spectra-Physics Argon laser beam ($\lambda = 514.5$ nm, operating at 40 mW) is incident on a hemispherical prism at the plasmon resonance angle θ_{ATR}. The samples are positioned on the top of the prism on the glass side with an index liquid (glycerol) of refractive index ($n = 1.474$ at $\lambda = 514.5$ nm) very close to ®pyrex one. Details of the experimental device have been presented and discussed elsewhere [17]. An horizontal micrometric shift of a planar mirror (M1) controls vertically the incidence of laser beam on the parabolic mirror (M2),
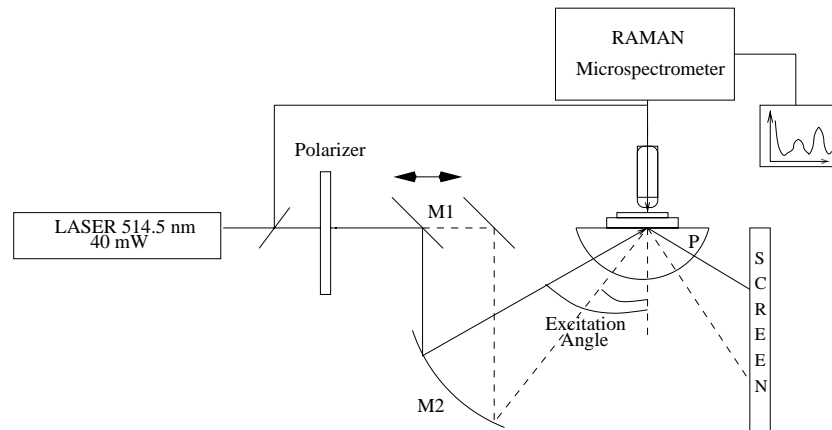
Fig. 6. Optical device used for the micro-Raman experiment.

so that it focuses precisely the light at the $silver$/ZrO_2 interface through the prism (P) and along the optical microscope axis. The light is then collected with the microscope objective of the Raman microspectrometer.

The main advantage [17] of micro-Raman spectroscopy experiment for such thin layer studies is that it is a non destructive analysis method, in comparison to TEM observations. The results of the micro-Raman spectroscopy experiments are shown in Figure 7. For the thinner film (sample B), no Raman bands can be distinguished from the background noise. For the thicker film (sample C), the spectrum exhibits wide bands at around 240, 459 and 640 cm^{-1}. The observed bands are assigned to the tetragonal ZrO_2 phase [22,24]. The broadness of the bands is due to the very small size of the particles, a few nanometers. Even though the Raman signal enhancement factor is about 85, the thickness (*e.g.* the low quantity of active sites) and probably the very weak Raman scattering cross section of ZrO_2 crystalline phase does not allow to obtain a significantly good signal for sample B. The fact, that the bands assigned to the monoclinic phase have not been observed, may have two reasons:

Firstly, we can assume that Raman scattering cross section of monoclinic phase is lower than tetragonal one. In this case, even though the proportion of monoclinic and tetragonal phase has not been determined by microscopy diffraction pattern study on which rings of each crystalline phase are clearly well-defined without noticeable intensity differences. We can conclude that the number of Raman active sites is lower than the one present in a film of the same thickness but only composed of tetragonal nanocrystallites. Raman scattering excited by surface plasmons seems to be a limited spectroscopic technic and has to be completed by microscopy studies. For materials as ZrO_2, thicknesses below 20 nanometers seems to be difficult to investigate only by Raman spectroscopy. Secondly, if we assume that the Raman scattering cross section of the monoclinic phase is at least equal to tetragonal one, it means that the proportion of monoclinic nanocrystals is very low. In this case, Raman scattering study can pro-
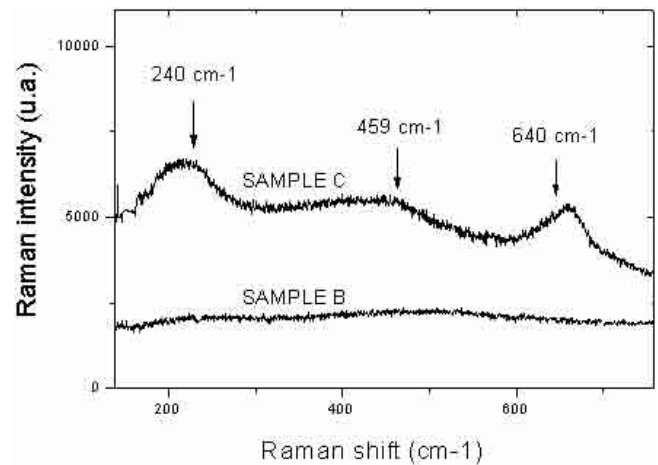

Fig. 7. Raman spectra of sample B and C.

vide informations about the dominant crystalline phase, and complete microscopy study. This last point confirms assumption that Raman scattering enhanced by SP_p can be proposed as a complementary structural analysis technique to Transmission Electron Microscopy observations.

Conclusion

This paper has illustrated an example of preparation of dense ultra thin films of ZrO_2 using the sol-gel route. The precise control of each annealing process step allows to obtain higher refractive indices than in thicker film case. The layer densification and nanocrystallization is realized by IR lamp heat treatment whereas the whole crystallisation is achieved by classical heating. CTEM and HRTEM studies coupled to micro-Raman spectroscopy enhanced by SP_p excitation, is proposed as an interesting complementary structural analysis technique for ultra thin films.

References

1. D.L. Jeanmaire, R.P. Van Duyne, J. Electro-anal. Chem. **84**, 1 (1977).
2. A. Otto, Surf. Sci. **72**, 392 (1978).
3. T.E. Furtak, J. Reyes, Surf. Sci. **93**, 35 (1980).
4. S.G. Schultz, M. Janik-Czachor, R.P. Van Duyne, Surf. Sci. **104**, 419 (1981).
5. Y.J. Chen, W.P. Chen, E. Burnstein, Phys. Rev. Lett. **36**, 1207 (1976).
6. K. Sakoda, K. Ohtaka, E. Hanamura, Solid State Commun. **41**, 393 (1982).
7. S. Ushioda, Y. Sasaki, Phys. Rev. B. **27**, 1401 (1983).
8. E. Kretschmann, A. Raether, Z. Naturf. **23a**, 2135 (1968).
9. W.P. Chen, J.M. Chen, J. Opt. Soc. Am. **71**, 189 (1981).
10. R.S. Sennett, G.D. Scott, J. Opt. Soc. Am. **40**, 203 (1950).
11. W.H. Weber, S.L. MacCarthy, Appl. Phys. Lett. **25**, 396 (1974).
12. C.J. Brinker, G.W. Scherer, *Sol-Gel Science* (Academic press, New York, 1990).
13. L. Klein, *Sol-Gel technology for thin films, fibers preforms, electronics and speciality shapes* (Noyes publication, 1988).
14. N. Tohge, K. Shinmou, T. Minami, J. Sol-Gel Sci. Tech. **2**, 251 (1994).
15. J.C. Debsikdar, J. Non-Cryst. Solids **86**, 231 (1986).
16. J.C. Plenet, A. Brioude, E. Bernstein, F. Lequevre, J.G. Dumas, J. Mugnier, Opt. Mater. **13**, 411 (2000).
17. A. Brioude, F. Lequevre, J. Mugnier, J. Dumas, G. Guiraud, J.C. Plenet, J. App. Phys. **88**, 6187 (2000).
18. B.E. Yoldas, Appl. Opt. **21**, 2960 (1982).
19. G. Teufer, Acta Crystal. **12**, 507 (1959).
20. R.F. Geller, P.J. Yavorsky, J. Res. Nat. Bur. Stand. **35**, 87 (1945).
21. N.J. Kreidel, J. Am. Ceram. Soc. **25**, 129 (1942).
22. C. Urlacher, J. Mugnier, J. Raman Spectroscopy **27**, 785 (1996).
23. A. Mehner, H. Klümper-Westkamp, F. Hoffmann, P. Mayr, Thin Solid Films **308-309**, 363 (1997).
24. M. Ishigame, T. Sakvrai, J. Am. Ceram. Soc. **60**, 367 (1977).